

## Proposed genetic model for the precipitation of uranium in Siwaliks of Taunsa area, D.G. Khan, Pakistan

ALTAF HUSSAIN, MUJEEB-UR-RAHMAN & M. A. SAMAD BAIG  
Pakistan Atomic Energy Commission, NMC-1 (DEU) D.G. Khan

**ABSTRACT:** *The fluvial rocks, mostly Siwaliks, comprise molasse sediments which are deposited during middle Miocene to Pleistocene. The middle Siwaliks of the area is the host rocks for uranium exploration in D.G. Khan Division. Two distinct types of ore deposits have been discovered so far in the Siwalik rocks of D.G.Khan, i.e. paleochannel type & chemical ore deposit.*

*The eastern limb of the Girdu anticline has a habit of rendering paleochannel type of ore deposits whereas the eastern limb of the Zinda Pir anticline is holding a unique type of uranium accumulation which may be termed as chemical ore body. This uranium accumulation has no corresponding radioactive signatures and the mineral accumulation appears to be quite young. The genetic model for this accumulation is interpreted as the secondary uranium which was formed along with fluvial sediments and got enriched due to subsurface water movement. The orogenic movements caused uplifting of these fluvial rocks due to which erosional surfaces developed. As a result, uranium got liberated through dissolution by water and was mobilized to the paleo-water tables. During episodic uplifts the process is repeated manifold and the last phase of uplifting has established the present day water table. Due to Eh-pH condition of the subsurface water, the remobilized uranium in the form of uranyl complexes reached the redox boundary (-ve Eh condition) where it changed its valency from U+6 to U+4 and got stabilized. Thus the stabilized U+4 precipitated at the redox interface due to change in Eh-pH conditions and formed chemical ore body. The Lal-Ashab uranium deposit of Taunsa is a similar ore accumulation which may be called as a hanging ore body existing at a depth of 45-50 m, 20 m below the present-day water table in a tabular shape. The mineral could not exactly be identified through ore microscopy and XRD, however, due to its young age the uranyl oxidized variety exists between U<sub>3</sub>O<sub>8</sub> & UO<sub>2</sub>. Some of the gamma logs show three levels of radioactivity which either show age difference or repeated mobilization scenario.*

### INTRODUCTION

The Siwalik Belt in the foothills of Sulaiman Range was known to host radioactivity all along its length. Taunsa, being a high dipping area, was never considered feasible for uranium exploration. Keeping the experience in Bannu Basin it was decided to explore this

area for remobilized type of uranium occurrence in the high dipping rocks of the Eastern Limb of Zinda Pir Anticline, Tanusa district (Fig. 1). The radiometric prospection resulted in the discovery of 4 radiometric horizons in middle Siwaliks strata, stacked one above the other between Sangar Nala and Mahoi Nala (Fig. 2).

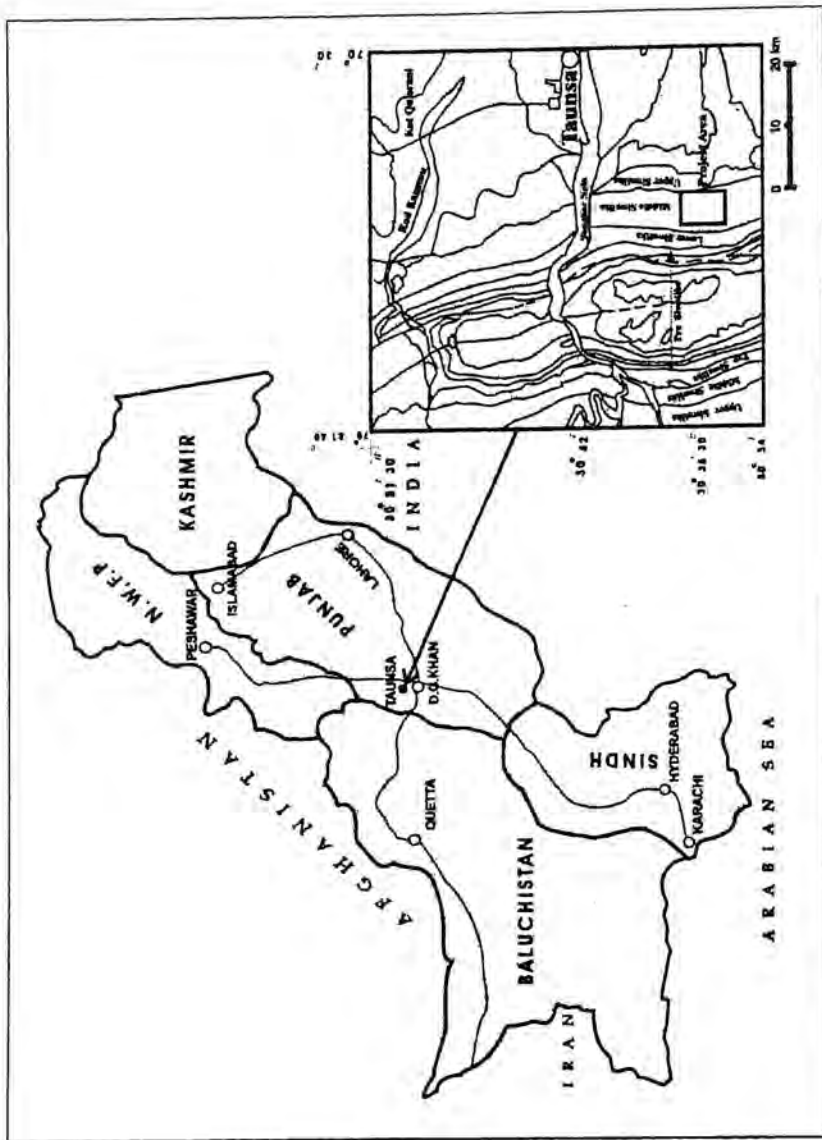


Fig. 1. Location map of Taunsa area, D.G. Khan.

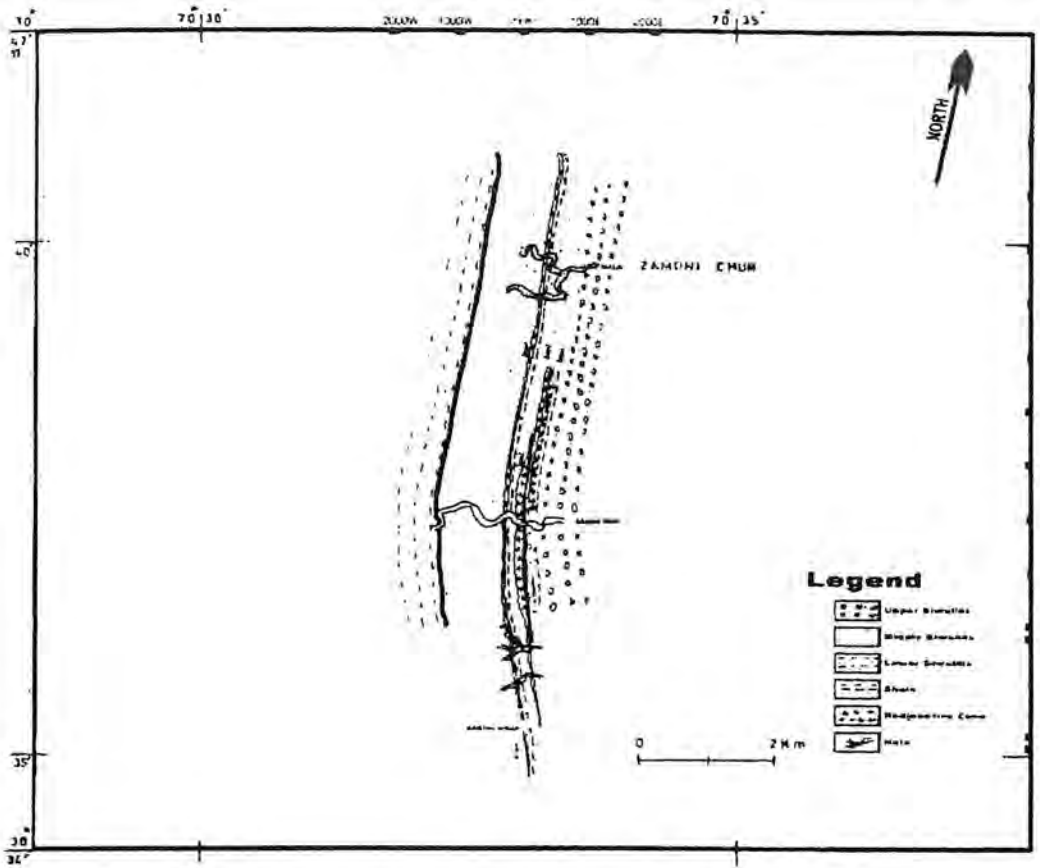


Fig. 2. Geological map of Taunsa area showing radioactive anomalous zones (Unpublished report of PAEC, D.G. Khan).

These radioactive horizons were named as:

1. Lal-Ashab uraniferrous horizon.
2. Fowl Creek uraniferrous horizon.
3. Zamdani uraniferrous horizon.
4. Ghazzi uraniferrous horizon.

All the horizons were sampled at various locations for chemical analysis of uranium mineralization. The microscopy and XRD method is CARNOTITE  $\{K_2(UO_2)_2V_2O_8\}$ .

#### REGIONAL TECTONIC FRAMEWORK

The Sulaiman lobe (Sarwar & DeJong, 1979) >300 km broad, lying to the southwest of the Himalayas is a tectonically active fold and thrust belt. The main structural elements in the Sulaiman fold belt are E-W trending arcuate, analyses depict (Table 1) that most of the radioactive surface samples are devoid of chemical uranium which indicate pronounced leaching phenomena. This tendency helps to explore the possibility of accumulation of chemical uranium as a result of leaching, mobilization and re-precipitation in the subsurface.

TABLE 1. ROCK SAMPLE ANALYSES COLLECTED FROM PROJECT AREA

| #  | Sample No. | Location (NGR) | Spot Reading CPS | Sample Reading CPS | U <sub>3</sub> O <sub>8</sub> % | Sample Description   |
|----|------------|----------------|------------------|--------------------|---------------------------------|--|
| 1  | Tau/Zdn-34 | 641803         | 2000             | 250                | < .01                           | Grey sandstone.  |
| 2  | Tau/Zdn-35 | 641803         | 5000             | 350                | < .01                           | Grey sandstone.  |
| 3  | Tau/Zdn-36 | 641803         | 2000             | 700                | < .01                           | Grey sandstone.  |
| 4  | Tau/Zdn-37 | 641801         | 400              | 400                | < .01                           | Grey sandstone.  |
| 5  | Tau/Zdn-38 | 641801         | 1100             | 175                | < .01                           | Grey sandstone.  |
| 6  | Tau/Zdn-39 | 641801         | 1100             | 150                | 0.012                           | Grey sandstone with clay balls.  |
| 7  | Tau/Zdn-40 | 641801         | 1800             | 170                | < .01                           | Grey sandstone with clay balls.  |
| 8  | Tau/Zdn-41 | 642799         | 2500             | 350                | 0.076                           | Grey sandstone having visible uranium mineralization.                      |
| 9  | Tau/Zdn-42 | 642799         | 3000             | 300                | 0.034                           | Grey sandstone having visible uranium mineralization.                      |
| 10 | Tau/Zdn-43 | 643798         | 5000             | 500                | 0.12                            | Grey sandstone having visible uranium mineralization alongwith clay balls. |
| 11 | Tau/Zdn-44 | 644794         | 2500             | 200                | 0.025                           | Grey sandstone having visible uranium mineralization.                      |
| 12 | Tau/Zdn-45 | 652800         | 100              | 60                 | 0.021                           | Grey sandstone having visible uranium mineralization.                      |

However, some of the radioactive rocks samples of the remanent ore body do have chemical uranium. The mineral of rock samples identified through ore convex to the south folds and faults which rotate rapidly to north-south direction along the margin of the active fold belt. Imbricate faults visible at the surface in the hinterland gradually disappear towards the deformation front (Hunting Survey Corporation, 1961; Kazmi & Rana, 1982). The Sulaiman fold and thrust belt is developed by transpression as a result of left lateral strike slip motion along the Chaman fault zone and southward thrusting along the western boundary of the Indian subcontinent (Sarwar & Lawrence et al., 1981; 1984).

The eastern Sulaiman Range is composed of the N-S trending Zinda Pir anticline in the

east and Girdu (Fort Munro) anticline in the west with Barthi-Baghal Chur syncline as the intervening basin (Wang et. al., 1996). Zinda Pir anticline which is also known as Zinda Pir anticlinorium (Iqbal & Ali, 1997) is a prominent structural element lying in the frontal part of the Sulaiman Fold belt. It comprises four main anticlines which from north to south are Dhodak, Rhodo, Afiband and Zinda Pir proper (Iqbal & Ali, 1997).

The 3rd Episode of the Himalayan Orogeny is characterized by the initiation and gradual development of Himalayan folded thrust belt, Sulaiman folded thrust belt and Chaman shear fault. Due to ongoing collision of the Indian and Eurasian Plates, a fore deep basin developed along the southern fringes of the Himalayan Orogenic belt and eastern most

part of the Sulaiman Fold and Thrust belt where uplifting Himalayas shed its erosional material. Actually this fore deep basin has controlled the initiation and development of the Paleo-Indus river system as well as the formation and layout of Siwalik rock series. The basin is now uplifted and deformed, representing the southward progression of Himalayan deformation.

Episode-IV of the Orogenic movement is the stage of strong compressional stresses forming the tectonic framework of the Sulaiman Range. During this episode N-S trending and plunging Zinda Pir anticline has also formed as a result of which the Paleo-Indus River has migrated and shifted further east to its present course of flow. Zinda Pir anticline runs parallel to the axis of Girdu anticline towards east and is separated by Barhi-Bagal chur - Sakhi Sarwar syncline. This Anticlinal zone marks the eastern boundary of the Sulaiman Fore deep. A complete conceptual diagram illustrating tectonic development of the Sulaiman uranium mineral belt during the Himalayan orogeny is given in Fig. 3 (Wang et al., 1996).

The investigated area is a part of the eastern flank of Zinda Pir anticline that exposes Siwaliks on eastern extremities of the Sulaiman Range. The Sulaiman Range in the area contains four terrace levels which are related to the last episode of Himalayan orogeny. These terraces represent paleopenepain levels which are related to eperiogenic periods within the last episode i.e. fifth episode.

## GEOLOGY OF PROJECT AREA

The uranium mineralization in the area occurs in fluvial sedimentary rocks of middle

Miocene to Quaternary ages, which make a part of middle Siwalik of the eastern Sulaiman Range. The Siwalik group comprises of Vihowa Formation (Lower Siwaliks), Litra Formation (Middle Siwaliks) and Chaudwan Formation (Upper Siwaliks). Siwaliks sequence represents diverse lithological and sedimentological features showing various phases of depositional environment. Lower Siwaliks predominantly consists of maroon to red claystone of sandy and silty nature inter-bedded with comparatively thick sandstone and reddish brown shale units.

The middle Siwaliks consist of a variety of sandstone units which are mostly thick bedded, however, thin hard bands of both epigenetic and syn-genetic nature and less frequent scouring surfaces are also present. These thin-bedded hard bands are in the form of clusters and commonly developed in upper part of the middle Siwaliks in a discontinuous fashion. Thick-bedded hard band are well continuous, highly calcified and most frequent in lower part. Shale to sandstone ratio is quite high in upper part, whereas shales are less common in lower part. The radiometric sandstone of the area is medium to coarse grained; at places gritty and greenish grey, mainly cross-bedded with abundant radiometric trash pockets and carbonaceous matter. Radioactive vertebrate fossils are uncommon. The contact between middle and lower Siwaliks is conformable and transitional.

Upper Siwaliks comprise pebble-conglomerates, coarse gritty sandstone and reddish brown shale units. The contact between middle and upper Siwaliks is conformable and gradational.

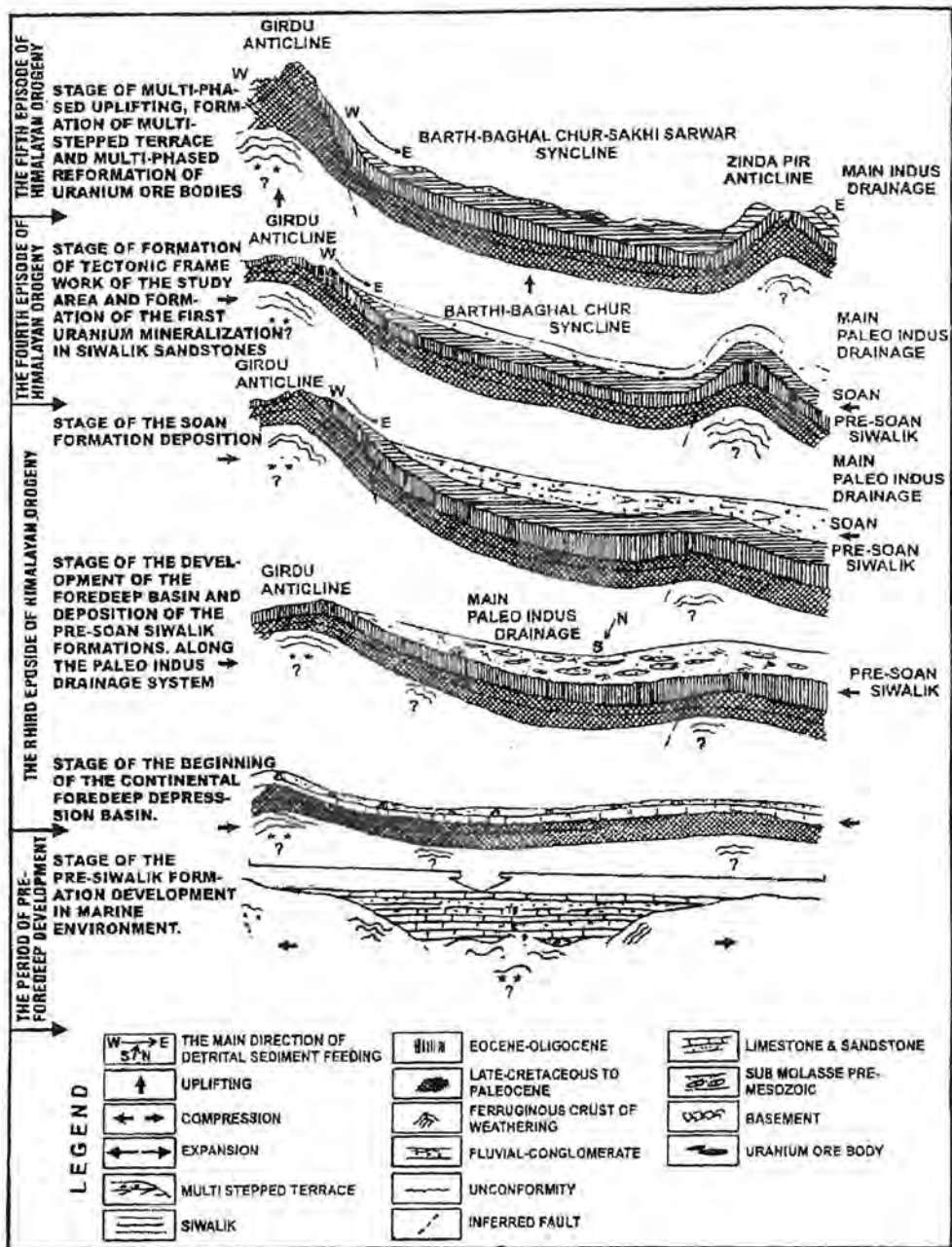


Fig. 3. A complete conceptual diagram illustrating tectonic development of the Sulaiman Uranium Mineral Belt during the Hima-Layan Orogeny (dimensions not to scale) (modified after Wang et al., 1996).

## GENESIS OF SUBSURFACE URANIUM ACCUMULATION IN THE AREA

The uranium accumulation is ribbon-shaped, tabular hanging structure that follows the strike direction. The width of surface radioactivity of uraniferous horizon is 30 m, but the subsurface width of uranium accumulation is up to 82 m i.e., the spread of uranium in the subsurface is more than the corresponding surface radiometry. The average thickness of the ore lenses is 5 meter. This uranium is remobilized / reworked, which is accumulated at the expense of leaching and remobilization of pre-existing surface anomalies at redox boundary that exists at a depth of 45-50 m, 20 m below the present day water table (Fig. 4).

A comparison of the character of the character of oxidation zone, transitional zone and reducing zone is given in Table 2 and 3. The subsurface uranium accumulation with weak radioactivity predicts the following working hypothesis. The sediments hosting the ore body were deposited in a fluvial environment with sufficient supplies of airborne volcanic matter & uranium from the primary rocks.

The uranium in this area is derived from syn-deposited volcanic ejecta in the form of volcanic ash falls and tuffs. The volcanics are more prone to enter into oxidized humid environment to liberate uranium. The liberation of uranium took place during diagenesis when these sediments were partially altered. This mobilized uranium got fixed with the carbon rich paleo-channel type sediments to form the initial ore body, which is still visible on the surface with grey clay balls, carbonaceous trash pockets and haematitized organic matter. As a result of orogenic movement, the sediments underwent intense folding due to which tectonic uplift of the area took place. The uranium got liberated through dissolution by ground water and was mobilized to the paleo water table. During periodic uplift the water table of the area repeatedly got lowered. The precipitated uranium had continuously been oxidized upon uplift and the redox boundary had gradually been shifted downward to the next stage contemporaneous to the phases of uplift. Gamma logs of the ore body represent three levels of uranium accumulation, which either show age difference or repeated mobilization-precipitation scenario. These three generation peaks indicate reprecipitation-remobilization phenomenon (Fig. 5).



Fig. 4. Conceptual diagram depicting the mode of leaching of uranium from the surface out crop and corresponding accumulation in the sub surface below ground water table.

TABLE 2. ROCK SAMPLES ANALYSES OF THE OXIDIZED ZONE

| #  | U <sub>3</sub> O <sub>8</sub> |                 |                 | Total Iron as Fe <sub>2</sub> O <sub>3</sub> | Ferrous Iron as FeO | Fe <sup>+2</sup> /Fe <sup>+3</sup> | Organic C | MoO <sub>3</sub> | V <sub>2</sub> O <sub>5</sub> |
|----|-------------------------------|-----------------|-----------------|--|---------------------|------------------------------------|-----------|------------------|-------------------------------|
|    | Chemical                      | U <sup>+4</sup> | U <sup>+6</sup> |  |                     |                                    |           |                  |                               |
|    | %                             | %               | %               |  |                     |                                    |           |                  |                               |
| 1  | <0.005                        | ---             | ---             | 5.730  | 0.041               | 0.007                              | ---       | ND               | 163.680                       |
| 2  | <0.005                        | ---             | ---             | 6.090  | 0.037               | 0.006                              | ---       | ND               | 247.700                       |
| 3  | 0.006                         | 0.0064          | ---             | 5.910  | 0.040               | 0.007                              | 0.360     | 4.790            | 99.490                        |
| 4  | <0.005                        | ---             | ---             | 5.710  | 0.042               | 0.007                              | ---       | 3.910            | 108.960                       |
| 5  | 0.005                         | 0.0039          | 0.0014          | 5.890  | 0.044               | 0.007                              | 0.360     | ND               | 139.290                       |
| 6  | <0.005                        | ---             | ---             | 7.340  | 0.049               | 0.007                              | ---       | 4.410            | 194.860                       |
| 7  | 0.007                         | 0.0074          | ---             | 4.770  | 0.033               | 0.007                              | 0.310     | 2.040            | 67.330                        |
| 8  | <0.005                        | ---             | ---             | 5.230  | 0.040               | 0.008                              | ---       | 2.750            | 60.570                        |
| 9  | <0.005                        | ---             | ---             | 5.510  | 0.041               | 0.007                              | ---       | 4.690            | 117.610                       |
| 10 | 0.007                         | 0.0074          | ---             | 5.780  | 0.040               | 0.007                              | 0.087     | 4.300            | 147.780                       |
| 11 | 0.006                         | 0.0039          | 0.0022          | 5.880  | 0.035               | 0.006                              | 0.083     | 3.950            | 116.850                       |
| 12 | 0.071                         | 0.0660          | 0.0050          | 5.440  | 0.036               | 0.007                              | 0.037     | 3.490            | 428.930                       |
| 13 | 0.024                         | 0.0150          | 0.0090          | 3.980  | 0.026               | 0.007                              | 0.033     | 2.680            | 121.310                       |
| 14 | 0.110                         | 0.0740          | 0.0360          | 4.670  | 0.032               | 0.007                              | 0.098     | 3.820            | 480.760                       |
| 15 | 0.015                         | 0.0150          | ---             | 4.740  | 0.044               | 0.009                              | 0.091     | 3.310            | 154.480                       |
| 16 | 0.008                         | 0.0082          | ---             | 5.210  | 0.053               | 0.010                              | 0.073     | 2.790            | 25.310                        |
| 17 | 0.006                         | 0.0057          | ---             | 5.940  | 0.057               | 0.010                              | 0.065     | 3.310            | 45.700                        |
| 18 | 0.016                         | 0.0160          | ---             | 6.730  | 0.060               | 0.009                              | 0.040     | ND               | 17.960                        |
| 19 | 0.010                         | 0.0095          | ---             | 6.660  | 0.059               | 0.009                              | 0.073     | 2.760            | 3.160                         |
| 20 | <0.005                        | ---             | ---             | 5.610  | 0.040               | 0.007                              | ---       | 6.320            | 480.590                       |
| 21 | <0.005                        | ---             | ---             | 5.500  | 0.037               | 0.007                              | ---       | 2.170            | 987.680                       |
| 22 | 0.008                         | 0.0081          | ---             | 5.050  | 0.037               | 0.007                              | 0.360     | ND               | 56.990                        |

TABLE 3 CORE SAMPLE ANALYSES OF TRANSITION AND REDUCING ZONE

| #  | Total Iron as Fe <sub>2</sub> O <sub>3</sub> % | Iron as FeO % | Vanadium as V <sub>2</sub> O <sub>5</sub> ppm | Carbon Organic as C % | Molybdenum as MoO <sub>3</sub> ppm | % U <sub>3</sub> O <sub>8</sub><br>(on dry basis) |
|----|--|---------------|---|-----------------------|------------------------------------|---|
|    |  |               |   |                       |                                    | Chemical  |
| 1  | 3.09   | 0.42          | 144.57  | 0.04                  | 14.39                              | 0.01  |
| 2  | 3.04   | 0.39          | 145.44  | 0.05                  | 19.93                              | 0.06  |
| 3  | 3.20   | 0.50          | 140.84  | 0.05                  | 19.48                              | 0.05  |
| 4  | 4.32   | 1.34          | 196.51  | 0.50                  | 18.22                              | 0.11  |
| 5  | 2.98   | 0.55          | 142.26  | 0.04                  | 2.03                               | 0.05  |
| 6  | 2.66   | 0.37          | 139.28  | 0.05                  | 1.50                               | 0.04  |
| 7  | 2.60   | 0.24          | 118.10  | 0.05                  | 1.70                               | 0.02  |
| 8  | 2.63   | 0.11          | 102.74  | 0.08                  | 1.87                               | 0.05  |
| 9  | 3.27   | 0.13          | 144.08  | 0.07                  | 2.30                               | 0.05  |
| 10 | 3.71   | 0.09          | 157.70  | 0.06                  | 1.00                               | 0.05  |
| 11 | 3.07   | 0.12          | 121.06  | 0.05                  | 1.52                               | 0.06  |
| 12 | 2.94   | 0.40          | 116.15  | 0.05                  | 1.00                               | 0.06  |
| 13 | 2.69   | 0.31          | 103.71  | 0.05                  | 3.42                               | 0.05  |
| 14 | 3.20   | 0.25          | 115.60  | 0.05                  | 2.26                               | 0.04  |

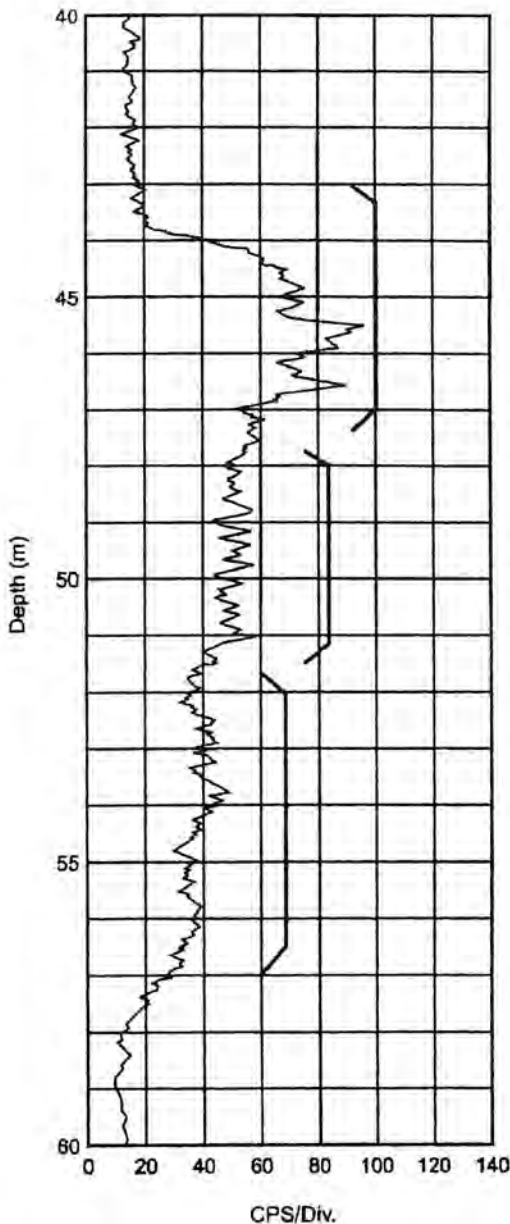


Fig. 5. Gamma Log of Taunsa area depicting three different levels of uranium accumulations.

The present day water table was established as a result of last episode of

uplifting. This water table has controlled the accumulation of uranium in the form of a hanging ore body. Hydrochemical character of the ground water is given in Table 4. The presence of free oxygen made the upper surface of water oxidized. With depth, oxygen become lesser and ultimately became non-existent thus the conditions became reducing that made Eh negative. The remobilized uranium, by reaching to redox boundary, changed its valency from +6 to +4 and got stable because U +4 is always stable in negative Eh conditions, and ultimately re-deposited there. The uranium ore, formed at the end of secondary mobilization is so young in age that no radioactivity is associated with it; this radioactive signature cannot be used for arithmetic assessment of the subsurface uranium ore body.

## CONCLUSIONS

The chemical ore body is emplaced as a result of trickling down of surface uranium mineralization available at expense of surface radiometry. The uranium accumulated below the ground water table, where Eh-pH conditions are favorable for precipitation. This ore body is formed at its present location through leaching, remobilization and accumulation at redox boundary. Gamma log of the ore body represent three levels of uranium accumulation, shows repeated mobilization-precipitation phenomenon. The uranium ore formed at the end of secondary mobilization is too young in age that no radioactivity is associated with it. Water samples collected from different holes of ore body indicates that pH remains slightly alkaline. The Eh versus pH conclude that the intersect lies in the area of slightly alkaline medium. During analysis of core samples it is observed that uranium is easily leachable with even fresh water and drilling mud.

TABLE 4. HYDROCHEMICAL CHARACTER OF THE PRESENT DAY GROUND WATER

| #  | Constituents                                     | samples<br>No.<br>W-1 | samples<br>No.<br>W-2 | samples<br>No.<br>W-3 | samples<br>No.<br>W-4 | samples<br>No.<br>W-5 | samples<br>No.<br>W-6 | samples<br>No.<br>W-7 | samples<br>No.<br>W-8 | samples<br>No.<br>W-9 | samples<br>No.<br>W-10 | samples<br>No.<br>W-11 | samples<br>No.<br>W-12 | samples<br>No.<br>W-13 |
|----|--|-----------------------|-----------------------|-----------------------|-----------------------|-----------------------|-----------------------|-----------------------|-----------------------|-----------------------|------------------------|------------------------|------------------------|------------------------|
| 1  | pH   | 7.710                 | 7.850                 | 7.820                 | 7.690                 | 7.710                 | 7.830                 | 7.700                 | 7.730                 | 7.790                 | 7.750                  | 7.750                  | 7.680                  | 7.840                  |
| 2  | Emf (mv)   | 221.900               | 211.500               | 211.500               | 211.400               | 211.900               | 2.10.0                | 215.100               | 214.600               | 214.500               | 219.400                | 213.900                | 211.700                | 207.300                |
| 3  | Temperature                                      | C°                    | 25.000                | 30.000                | 30.000                | 30.000                | 32.000                | 30.000                | 30.000                | 30.000                | 30.000                 | 30.000                 | 29.000                 | 30.000                 |
| 4  | Uranium as<br>U <sub>3</sub> O <sub>8</sub>      | ppm                   | 0.370                 | 0.370                 | 0.330                 | 0.340                 | 0.260                 | 0.280                 | 0.390                 | 0.400                 | 0.400                  | 0.360                  | 0.380                  | 0.320                  |
| 5  | Bicarboante<br>as HCO <sub>3</sub> <sup>-1</sup> | ppm                   | 218.700               | 218.700               | 218.700               | 218.700               | 218.700               | 218.700               | 230.180               | 218.700               | 218.700                | 218.700                | 218.700                | 230.210                |
| 6  | Sulphate as<br>SO <sub>4</sub> <sup>-2</sup>     | ppm                   | 274.510               | 245.850               | 254.900               | 260.180               | 257.920               | 266.210               | 261.990               | 276.770               | 288.840                | 286.580                | 289.590                | 232.280                |
| 7  | Chloride Cl <sup>-1</sup>                        | ppm                   | 40.000                | 36.000                | 36.000                | 32.000                | 32.000                | 34.000                | 34.000                | 34.000                | 36.000                 | 32.000                 | 34.000                 | 32.000                 |
| 8  | Calcium as<br>Ca <sup>+2</sup>                   | ppm                   | 76.950                | 66.530                | 65.730                | 65.730                | 65.730                | 65.730                | 67.330                | 67.330                | 70.540                 | 68.930                 | 70.540                 | 57.720                 |
| 9  | Magnesium<br>Mg <sup>+2</sup>                    | ppm                   | 43.770                | 39.400                | 39.880                | 40.860                | 40.370                | 41.340                | 41.830                | 42.800                | 42.800                 | 41.830                 | 46.690                 | 35.510                 |
| 10 | Sodium as<br>Na <sup>+1</sup>                    | ppm                   | 70.190                | 70.190                | 72.120                | 75.960                | 78.850                | 80.770                | 81.770                | 85.580                | 88.460                 | 88.460                 | 93.270                 | 80.770                 |
| 11 | Potassium<br>as K <sup>+1</sup>                  | ppm                   | 14.850                | 8.510                 | 5.520                 | 7.010                 | 7.420                 | 7.200                 | 7.420                 | 7.390                 | 7.570                  | 7.800                  | 7.910                  | 6.720                  |
| 12 | Silica as<br>SiO <sub>2</sub>                    | ppm                   | 14.210                | 14.010                | 14.060                | 13.820                | 14.020                | 13.890                | 13.690                | 13.750                | 13.430                 | 13.130                 | 13.280                 | 13.650                 |
| 13 | Iron as<br>Ferrous Fe <sup>+2</sup>              | ppm                   | 0.570                 | 0.510                 | 0.110                 | 0.020                 | 0.730                 | 0.092                 | 0.074                 | 0.130                 | 0.110                  | 0.330                  | 0.280                  | 0.074                  |
| 14 | Iron as<br>Ferric Fe <sup>+3</sup>               | ppm                   | 0.110                 | 0.140                 | 0.140                 | 0.057                 | 0.077                 | 0.058                 | 0.066                 | 0.070                 | 0.060                  | 0.100                  | 0.060                  | 0.076                  |
| 15 | Iron Total<br>as Fe                              | ppm                   | 0.680                 | 0.650                 | 0.250                 | 0.077                 | 0.150                 | 0.150                 | 0.140                 | 0.200                 | 0.170                  | 0.430                  | 34.000                 | 0.150                  |

## REFERENCES

- Hunting Survey Corporation, 1961. Reconnaissance Geology of part of West Pakistan. A Colombo plan cooperation project. Government of Canada, Geodynamics, Toronto.
- Iqbal, M. & Ali, S.M. 1997. A possible role of strike slip fault related tectonics in the development of Zindapir anticlinorium, Pakistan. Unpubl. Rep. Hydroc. Inst. Pakistan.
- Lawrence, R. D., Khan, S.H., Dejong, K.A., Farah, A. & Yeats, R.S., 1981. A thrust and strike slip fault interaction along Chaman fault zone, Pakistan, In: Thrust and nappe Tectonics (K.R. Maclay & N.J. Price, eds.), Geol. Soc. London, Spec. Publ., 363-370.
- Sarwar, G., & Dejong, K.A., 1979. Arcs, Oroclines, syntaxes. The Curvature of mountain belts in Pakistan. Geodynamics of Pakistan, Geol. Surv. Pak., Quetta.
- Wang, Z.B., Tang, S.G., Chen, D. & Nie, F., 1996. Basic geological studies and preliminary evaluation of uranium potential of Siwaliks in the middle part of Sulaiman mineral belt Pakistan. Unpubl. PAEC Report.